Positive Aspects of Negative Design: Simultaneous Selection of Specificity and Interaction Stability †

ARTICLE *in* BIOCHEMISTRY · APRIL 2007

Impact Factor: 3.02 · DOI: 10.1021/bi602506p · Source: PubMed

3 AUTHORS:

Jody M Mason
University of Bath
36 PUBLICATIONS **1,251** CITATIONS
SEE PROFILE

Kristian M. Müller
Bielefeld University
52 PUBLICATIONS **1,285** CITATIONS
SEE PROFILE

Katja M. Arndt
Universität Potsdam
60 PUBLICATIONS **1,737** CITATIONS
SEE PROFILE

Positive Aspects of Negative Design: Simultaneous Selection of Specificity and Interaction Stability†

Jody M. Mason, Kristian M. Müller, and Katja M. Arndt*

Institute of Biology III, Albert-Ludwigs University of Freiburg, Schänzlestrasse 1, D-79104 Freiburg, Germany

Received December 5, 2006; Revised Manuscript Received February 6, 2007

ABSTRACT: The energetic determinants that drive specific protein−protein interactions are not entirely understood. We describe simultaneous *in vivo* selection of specific and stable interactions using homologous peptides which compete with protein libraries for an interaction with a target molecule. Library members binding to their target, and promoting cell growth, must outcompete competitor interactions with the target (i.e., competition) and evade binding to the competitors (i.e., negative design). We term this a *competitive and negative design initiative* (CANDI). We combined CANDI with a *protein-fragment complementation assay* (PCA) and observed major specificity improvements, by driving selection of winning library members that bind their target with maximum efficacy, ensuring that otherwise energetically accessible alternatives are inaccessible. CANDI−PCA has been used with libraries targeted at coiled coil regions of oncogenic AP-1 components cJun and cFos. We demonstrate that comparable hydrophobic and electrostatic contributions in desired species are compromised in nondesired species when CANDI is executed, demonstrating that both core and electrostatic residues are required to direct specific interactions. Major energetic differences (≥5.6 kcal/mol) are observed between desired and nondesired interaction stabilities for a CANDI−PCA derived peptide relative to a conventional PCA derived helix, with significantly more stability (3.2 kcal/mol) than the wild-type cJun−cFos complex. As a negative control, a library lacking a residue repertoire able to generate a specific and stable helix was tested. Negative protein design has broad implications in generating specific and therapeutically relevant peptide-based drugs, proteins able to act with minimal cross-talk to homologues or analogues, and in nanobiotechnological design.

Understanding how protein−protein interactions evolve to avoid the formation of alternative or pathogenic species is a fascinating biological enigma. These interactions usually occur in a crowded intracellular environment with many competing homologues present (*1*). Affinity and concentration control the equilibrium stability of the desired species, as does the free energy of binding to other molecules. An understanding of the molecular processes underpinning this affinity and specificity is crucial in understanding how protein networks function. Designing peptide based inhibitors to bind with both high affinity and specificity to pathogenic proteins implicated in disease is of utmost importance, and promises to yield important rules. Until recently, however, experimentalists have been largely restricted to designing in the positive (desirable) direction. Designed inhibitors arising from this "single-state" approach may meet their objective in binding to their target with desired affinity. However, the advantage of an *in vivo* derived inhibitor is its increased specificity for that target. This so-called negative or "multistate" design is key to deriving high affinity yet specific peptide-based drugs.

We have focused on the coiled coil system as it is simplistic, but highly specific, being ubiquitous and important for many biological processes; found in 3−5% of the entire coding sequence (*2*) it serves in transcriptional control (*3*), muscle contraction (*4*), viral infection (*5*, *6*), cell signaling (*7*), molecular chaperones (*8*), and fertilization (*9*), and is therefore the ideal test-bed on which to test specificity. In addition, many of the rules arising from interactions involving coiled coils are also applicable to other protein−protein interactions. Coiled coils are characterized by a regular repeating unit of seven amino acids (a heptad repeat) labeled ***a***−***g***, with a specific pattern of hydrophobic and hydrophilic residues. Specific details have been discussed extensively elsewhere (*10*−*18*).

The Jun and Fos coiled coil proteins from the mammalian transcription factor activator protein-1 (AP-1[1]) consist of a variety of cellular homologues which are expressed in different tissues, leading to increased levels of proliferation, invasion, and metastasis when upregulated (*19*). A variety of oncogenic signaling pathways converge on AP-1 which ultimately controls gene expression patterns (*20*). Accordingly, designing inhibitors to sequester specific AP-1 components is of great interest for analytical as well as therapeutic purposes. Such inhibitors were derived using a semirational library approach combined with a protein-fragment complementation assay (PCA) for selecting library

† This work was funded in the Emmy Noether program of the Deutsche Forschungsgemeinschaft (Grant Ar 373/1-1, 1-2).

* Address correspondence to this author. Tel: +49-761-203-2748. Fax: +49-761-203-2745. E-mail: Katja@biologie.uni-freiburg.de.

[1] Abbreviations: CANDI, competitive and negative design initiative; DHFR, dihydrofolate reductase; PCA, protein-fragment complementation assay; AP-1, activator protein-1.

10.1021/bi602506p CCC: $37.00
Published on Web 04/03/2007

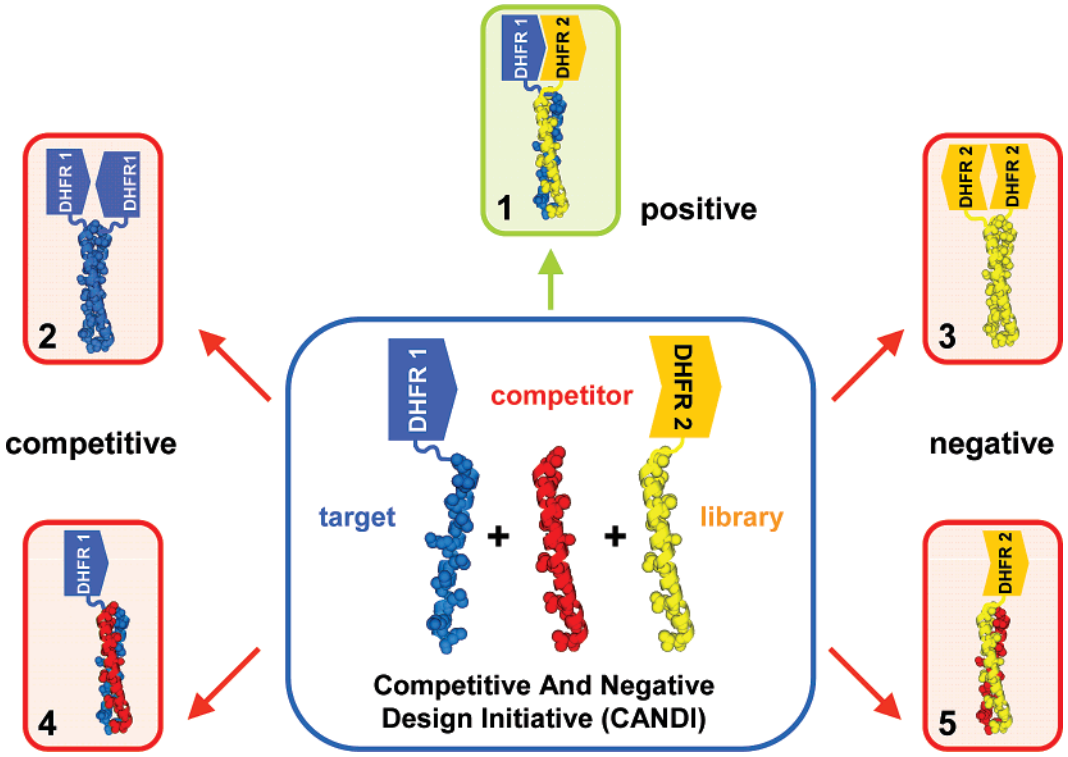

FIGURE 1: Conceptual diagram highlighting the "*competitive and negative design initiative*" (CANDI) which has been applied using the "*protein-fragment complementation assay*" (PCA) system. Only favorable and specific interactions between a library member (gold) and target (blue) will reconstitute the DHFR enzyme and thus will give rise to a bacterial colony under selective conditions (outcome 1). How the PCA assay works is explained in brief in Materials and Methods, and in more detail elsewhere (*21*, *25*−*30*). Conventional PCA already disfavors homodimers (outcomes 2 and 3), whereas CANDI−PCA enhances this effect by including additional constraints. Specifically, library members that have a lower binding constant for the target than the target−competitor interaction (outcome 4) or that bind preferentially to the competitor (red; outcome 5) are detrimental inhibitors and will result in no or retarded cell growth. In the case of low affinity binding (a combination of outcome 1 with undesired outcomes 2 and/or 4) or nonspecific binding (a combination of 1 with 3 and/or 5), the colony will be outgrown in subsequent growth competitions by library members of comparable or better affinity, but higher specificity (see also introduction).

members with highest affinity. In PCA, one half of murine dihydrofolate reductase (mDHFR) is genetically fused to the target, and the second half of mDHFR is fused to the protein library. Only library members binding to the peptide target will bring the two halves of DHFR together, render the enzyme active, and result in a bacterial colony under selective conditions. Subsequent growth competition under selective conditions enriched two "winning" peptides, termed FosW and JunW, targeting cJun and cFos, respectively (*21*). These 37-mer peptides were analyzed regarding both their stabilities and specificities. The new dimeric coiled coils, cJun−FosW and JunW−cFos, displayed remarkable T_m values of 63 °C and 44 °C, compared to only 16 °C for wild-type cFos−cJun, thus fulfilling the criteria of higher stability. Unfortunately other undesired complexes showed similar or even higher T_m values (e.g., cFos−FosW, T_m = 61 °C; cJun−JunW, T_m = 57 °C). We predicted that in order to increase binding specificity one must maximize unfavorable interactions in competing states and favorable interactions in the target conformation, while maintaining intramolecular stability.

To increase interaction specificity, we added homologous competitors to the PCA system. In this new system, library members must not only bind their target (positive design) but also bind it with higher affinity than the competitor (competition) and also evade binding to the competitor itself (negative design) (Figure 1). Consequently, we term this a "*competitive and negative design initiative*" (CANDI). To demonstrate *in vivo* negative design, we combined CANDI with PCA selection, where non-DHFR-fragment fusions of cFos or cJun are used to compete with libraries, to bind to Jun and Fos target peptides (Figure 1). Other dual positive−negative selection systems have been described (*22*, *23*). However, to our knowledge this is the first *in vivo* negative design library selection, which, in principle, is amenable to any protein−protein interaction as PCA has been established in various organisms, and CANDI is also transferable to other selection systems. It should be emphasized that CANDI−PCA can only be as successful as the residue options and positions open to it; these must be able to confer a stable desired interaction and simultaneously exclude formation of alternative nondesired species. Sequence inspection of our libraries predicted the cJun-based library to have sufficient residue options to generate a winner specific for its cFos target. Conversely, the cFos-based library was predicted to have insufficient residue options to be both stable and specific for its cJun target, and was thus included as a negative control. This Fos library negative control is informative because it demonstrates that additional specificity using CANDI−PCA can only be achieved when suitable amino acid options are available.

To directly compare CANDI−PCA with conventional PCA, previously designed libraries were used (*21*). Stability differences for desired and undesired coiled coils, with and without negative design, provide a rigorous test of the CANDI−PCA implementation. This is important in ruling

out specificity as a byproduct of optimizing for complex stability alone (*24*). Five outcomes (or a combination of) are feasible (Figure 1):

1. The library member binds specifically and with high affinity to the target (positive state).

2. The library member cannot compete with target homodimerization (competitive state).

3. The library member preferentially homodimerizes rather than binding to the target (negative state).

4. The library member cannot outcompete target−competitor interaction (competitive state).

5. The library member preferentially binds the competitor rather than the target (negative state).

PCA has a crude level of negative design by selecting against intracellularly expressed proteins competing for an interaction (*21*, *25*−*30*). Further, homodimerization of both target (outcome 2) and library members (outcome 3) competes against the desired target−library member interaction (outcome 1). CANDI−PCA increases selection pressure by including outcomes 4 and 5. Since the competitor is not fused to a DHFR fragment, outcomes 4 and 5 will not result in restored DHFR activity and transformed cells will be depleted, removing the library members. In contrast, a combination of outcome 1 (the positive state) with outcomes 4 and 5 would give rise to a colony under selective conditions but would be predicted to be outgrown in subsequent growth competitions by library members binding with high affinity and specificity to the target (outcome 1). In a cellular context, outcome 5 represents sequestration of a protein behaving normally in isolation, but possibly leading to undesired side effects in a cellular context. This could render a cancerous situation even more oncogenic. Here, we demonstrate that, depending on the library options, the additional constraints of the "*competitive and negative design initiative*" (CANDI) in the PCA selection can significantly increase interaction specificity. Analysis of these factors helps to understand how nature achieves specificity, and derived peptides targeting AP-1 are promising tools for analytical as well as biomedical purposes.

MATERIALS AND METHODS

Library Design and Cloning. Library design and cloning has been described elsewhere (*21*). Briefly mega-primers were synthesized including relevant degenerate codons for library residue options, and a fill-in reaction performed, resulting in 111 bp double stranded oligonucleotides. These were cloned via *Nhe*I and *Asc*I sites into a pQE16 derivative (Qiagen) containing a G/S linker tagged to fragment 1 (pAR230d; cJun and Jun library; ampicillin resistance [K.M.A., unpublished data]) or fragment 2 (pAR300d; cFos and Fos library; chloramphenicol resistance [K.M.A., unpublished data]) of murine dihydrofolate reductase (mDHFR) respectively. Competing helices were cloned into a third plasmid (pAR410d (*21*); tetracycline resistance) via *Xho*I and *Asc*I and consequently lacked a DHFR fragment fusion. All proteins were under control of a lac promoter, and expression was induced with isopropyl β-D-1-thiogalactopyranoside (IPTG). In the case of conventional PCA, library plasmids were transformed into BL21 cells (Stratagene) containing target plasmid and pREP4 (Qiagen; for lac repression; kanamycin resistance). In the case of CANDI−PCA, the fourth competing helix plasmid was also transformed. To assess library quality we sequenced pools and single clones and found approximately equal distributions of varied amino acids. Pooled colonies exceeded the library size 5−10-fold.

Selection of Winner Peptides. The protein-fragment complementation assay has been described in detail elsewhere (*25*, *27*, *28*). Briefly, target and library peptides are tagged at the genetic level to either half of mDHFR. Only two interacting helices will bring the two halves of the enzyme into close proximity, render the enzyme active, and result in colony formation on M9 minimal medium plates with 1 μg/mL trimethoprim to inhibit bacterial DHFR. The third competing peptide is expressed on a plasmid conferring tetracycline resistance but is not fused to a DHFR fragment. Hence, preferential binding of this competing helix to either the target or the library member will not give rise to a colony under selective conditions. Surviving colonies were pooled, grown, and serially diluted in liquid cultures under selective conditions (M9 minimal medium with 1 μg/mL trimethoprim). Fastest growth, and hence the highest affinity interacting partners, dominated the pool. Library pools as well as colonies from individual clones were sequenced to verify the arrival at one sequence.

Peptide Synthesis and Purification. Peptides were synthesized by Protein Peptide Research Ltd, Eastleigh, U.K., and subsequently purified to over 98% purity using RP-HPLC with a Jupiter Proteo column (4 μm particle size, 90 Å pore size, 250 × 10 mm; Phenomenex) and a gradient of 5−50% acetonitrile (0.1% TFA) in 50 min at 1.5 mL/min. Correct masses were verified by electrospray mass spectrometry.

The peptides cJun (ASIARLEEKVKTLKAQNYELASTANMLREQVAQLGAP), cFos (ASTDTLQAETDQLEDEKYALQTEIANLLKEKEKLGAP), JunW (ASAAELEERVKTLKAEIYELQSEANMLREQIAQLGAP), FosW (ASLDELQAEIEQLEERNYALRKEIEDLQKQLEKLGAP), JunW_{CANDI} (ASAAELEERAKTLKAEIYELRSKANMLREHIAQLGAP), and FosW_{CANDI} (ASLDELQAEIEQLEDQNYALQKEVEDLRKELEKLGAP) were amidated and acetylated and contained N- and C-capping motifs (underlined) for improved helix stability and solubility. Peptide concentrations were determined in water using absorbance at 280 nm with an extinction coefficient of 1209 M^{-1} cm^{-1} (*31*) corresponding to a Tyr residue inserted into a solvent exposed ***b3*** heptad position.

Circular Dichroism Measurements. Spectra and thermal melts were performed at 150 μM total peptide concentration in 10 mM K-phosphate, 100 mM KF, pH 7, using a Jasco J-810 CD instrument. The temperature was ramped at a rate of 0.5 °C/min. Melting profiles were ≥94% reversible with equilibrium denaturation curves fitted to a two-state model to yield the melting temperature (T_m):

$$\Delta G = \Delta H - (T_A/T_m) \times (\Delta H + R \times T_m \times \ln(P_t)) + \Delta C_p \times (T_A - T_m - T_A \times \ln(T_A/T_m)) \quad (1)$$

where ΔH is the change in enthalpy, T_A is the reference temperature; R is the ideal gas constant, P_t is the total peptide concentration, and ΔC_p is the change in heat capacity. Melting profiles for heterodimers are clearly distinct from averages of constituent homodimeric melts, indicating that helices are dimerizing in an apparent two-state process. Protein folding studies have demonstrated that for GCN4, a

Table 1: Thermal Unfolding Data Derived from Circular Dichrosim Studies

	T_m values						ΔT_m values[a]	
	cJun	cFos	JunW	$JunW_{CANDI}$	FosW	$FosW_{CANDI}$	JunW related	FosW related
cJun	24	16	57	23	63	52	23 − 57 = −34	52 − 63 = −11
cFos		−1	44	44	61	50	44 − 44 = 0	50 − 61 = −11
JunW			66				29 − 66 = −37	
FosW					57			45 − 57 = −12
$FosW_{CANDI}$						45		
$JunW_{CANDI}$				29				
$\Delta\Delta T_m$ values[b]							0 − (−34) = 34	−11 − (−11) = 0

[a] ΔT_m (°C) values demonstrate the drop in T_m (derived from the fits in Figure 3) for species with competitive negative design strategy relative to conventional PCA. [b] $\Delta\Delta T_m$ values can be calculated from the respective ΔT_m values (e.g., 0 − (−34) = 34).

yeast homologue of AP-1, both binding and dissociation of dimers are tightly coupled with folding/unfolding of the individual helices, and are described by a simple two-state model (*32*, *33*). The melting transitions are concentration dependent, indicative of a dimeric interaction. E.g. native gel electrophoresis showed that the heterotypic $JunW_{CANDI}$−cFos is clearly favored over $JunW_{CANDI}$−$JunW_{CANDI}$ or cFos−cFos. The only instance where more than one species has been observed is for the combination of cJun−$JunW_{CANDI}$ (as seen in the native gel). Consequently, the free energy derived from this thermal melt is perhaps less accurate than for others. Further proof that a mixture of helices exchange to the most stable scenario ($JunW_{CANDI}$−cFos) is demonstrated in Figure 5. The corresponding two-state transitions which are observed for the heterodimers are distinct from the homodimers, and a mixture of four different possible dimers is not observed. For homodimers and heterodimers to exchange and appear as an apparent two-state process would require them to have extremely close T_m values in the first instance, which would have little bearing on the difference in observed T_m for either dimer.

Additionally, ΔT_m values given in Table 1 are calculated using $\Delta T_{m(CANDI-No\ CANDI)} = T_{m(CANDI)} - T_{m(No\ CANDI)}$), and $\Delta\Delta T_m = [T_{m(CANDI)} - T_{m(No\ CANDI)}] - [T_{m(COMPETITOR\ with\ CANDI)} - T_{m(COMPETITOR\ without\ CANDI)}]$. E.g. $\Delta T_{m(cFos-JunWCANDI\ -\ cFos-JunW)} = T_{m(cFos-JunWCANDI)} - T_{m(cFos-JunW)} = 44\ °C - 44\ °C = 0\ °C$; $\Delta\Delta T_m = [T_{m(cFos-JunWCANDI)} - T_{m(cFos-JunW)}] - [T_{m(cJun-JunWCANDI)} - T_{m(cJun-JunW)}] = [44\ °C - 44\ °C] - [23\ °C - 57\ °C] = 34\ °C$. Additionally calculated differences between coiled coil values at 37 °C reported in Krylov et al. (*34*) and Acharya et al. (*35*) remain as $\Delta\Delta G$ rather than $\Delta\Delta\Delta G$ due to cancellation of the ground states. In these publications both ***a/a′*** and ***g/e′*** stabilities are calculated relative to an alanine−alanine pair (A ↔ A; e.g., $\Delta\Delta G_{Q\leftrightarrow E}$ relative to $\Delta\Delta G_{Q\leftrightarrow Q} = [\Delta G_{Q\leftrightarrow E} - \Delta G_{A\leftrightarrow A}] - [\Delta G_{Q\leftrightarrow Q} - \Delta G_{A\leftrightarrow A}] = \Delta G_{Q\leftrightarrow E} - \Delta G_{Q\leftrightarrow Q} = \Delta\Delta G_{QE\leftrightarrow QQ}$). It should be noted that these values have been averaged from the data reported for ***g/e***$_{i+1}$ and ***e′***$_{i+1}$***/g***; distinguishing between ***e*** and ***g*** did not improve the data set.

Native Gel Analysis. Samples of individual peptides as well as equimolar mixtures were diluted 2-fold in 0.2% (w/v) methyl green, 20% glycerol, 500 mM β-alanine acetate, pH 3.8. The peptides were loaded to a concentration of 600 μM (~24 μg). Gels contained 7.5% acrylamide in 375 mM β-alanine acetate, pH 3.8. The gel was prerun for 1 h, samples were loaded, and the gel was run for a further 3 h at 100 V. During this time it was necessary to reverse the electrodes so that the protein sample ran to the anode. Gels were fixed with 2% glutaraldehyde and stained overnight in 0.2% Coomassie brilliant blue (R-250), 20% acetic acid, before destaining in the same solvent lacking the dye. The caluculated overall positive charge of the peptides at pH 3.8 (Protein Calculator v3.3; http://www.scripps.edu/~cdputnam/protcalc.html) was as follows: cFos = 2.4, cJun = 4.4, JunW = 2.8, $JunW_{CANDI}$ = 6.0.

Comparison of Thermal and Chemically Derived Free Energy Values. Thermal T_m data were converted to generate ln $K_{D(temp)}$ values, by calculating K_D values from fraction folded and unfolded in the transition region and linear extrapolation to the reference temperature. To account for inaccuracies due to the temperature dependence of ΔH, we converted these ln $K_{D(temp)}$ values to ln $K_{D(urea)}$ values at a reference temperature of 20 °C according to the relationship

$$\ln K_{D(urea)} = (\ln K_{D(temp)} - 0.3222)/1.1982 \qquad (2)$$

This equation is explained in detail in the supporting information elsewhere (*21*) and is used to relate core and electrostatic energy free energy changes reported in the literature (*34*, *35*) to the change in free energy derived from thermal unfolding data. For comparison with published data we considered various temperatures and found $\Delta\Delta G$ to be consistent over the required temperature range.

RESULTS

Previously designed libraries directed at cJun and cFos were screened for peptides binding their targets with high affinity and specificity by implementing a "*competitive and negative design initiative*" (CANDI) into the "*protein-fragment complementation assay*" (PCA) system. Interfacial contact residues in designed libraries (Figure 2A for Jun library, Figure 2D for Fos library; see legend for schematic explanation) were varied to give a range of potential interactions in the selected molecule. Semi-rational design included residues known to confer to a high stability complex as well as residues that, if selected, would be novel and therefore highly informative. It should be noted that, for short dimeric coiled coils, folding and binding are tightly coupled processes (*32*, *36*), and references here to the stability of the complex also includes the binding affinity of the interaction. The two following sections provide detailed descriptions of the libraries, the selection outcome, and the differences between PCA and CANDI−PCA selected helices. Rules emerging from such experimental studies can speed the path to a species which is both specific and stable.

Helical wheel inspections of previously selected PCA winning sequences with target and homologue peptides demonstrated comparable edge electrostatics and core hy-

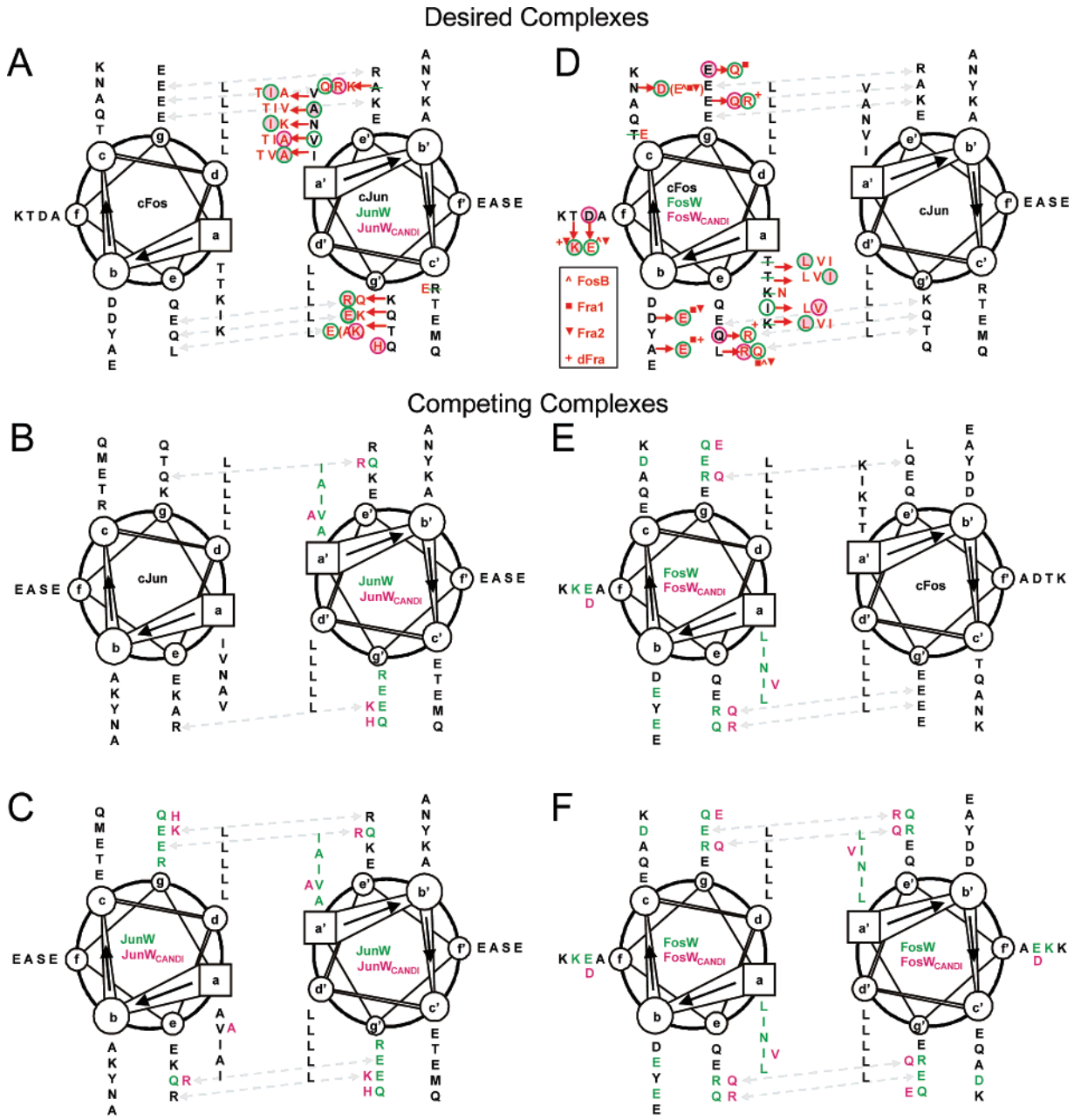

FIGURE 2: Schematic representation of desired and competing complexes for the AP-1 coiled coil. The helical wheel diagram looks down the axis of the α-helices from N- to C-terminus, and illustrates the attractive and repulsive forces which prevent and maintain specificity in the cases of JunW$_{CANDI}$ and JunW, respectively. In these diagrams, parallel dimeric helices are shown and contain hydrophobic residues at the dimeric interface (***a***/***d***) of the heptad repeat and electrostatic residues flanking these positions (***e***/***g***). CANDI is implemented by including close homologues of both target and library to the screening process but lacking a DHFR fragment fusion (B,C and E,F). Consequently, if either target or library member binds to the homologue, then the library member is either not specific, or stable, in binding its target (Figure 1). Black represents residues found in all peptides; red represents library options; residues circled in green (A and D) and green residues (B,C and E,F) represent residues selected in JunW, JunW$_{CANDI}$, FosW, or FosW$_{CANDI}$; residues circled in magenta (A and D) and magenta residues (B,C and E,F) represent selections that are unique to JunW$_{CANDI}$ or FosW$_{CANDI}$.

drophobic interactions for both desired (Figure 2A and 2D) and alternative species (Figure 2B,C and 2E,F). Closer inspection of the library options indicated that the Jun library had the potential to yield a sequence binding cFos while simultaneously disfavoring cJun binding. Conversely, inspection of the Fos library indicated that it was unlikely to have the necessary residue repertoire to select a binder for cJun while simultaneously selecting against cFos.

The Jun and Fos libraries therefore represented ideal testbeds for positive and negative controls, respectively. Screening indeed identified two winning sequences, termed JunW$_{CANDI}$ and FosW$_{CANDI}$. Importantly, the libraries used in both instances are the same as those used in a previous publication (*21*), with differences in the winning sequences (Figure 2) revealing the effect of CANDI on PCA selection.

Differences between JunW and JunW$_{CANDI}$. The coiled coil region of cFos was used as target. The library had a total of ten ***a***, ***e***, and ***g*** positions varied, with ***b***, ***c***, ***d***, and ***f*** heptad positions of cJun used as the template. This library has been discussed in depth previously (*21*). Briefly, Thr, Ile, Val, and Ala options were introduced at ***a*** positions (see Figure 2A), thereby retaining all wild-type residue options while introducing varying amounts of hydrophobic bulk to the side-chain options. cJun ***e*** positions that are largely

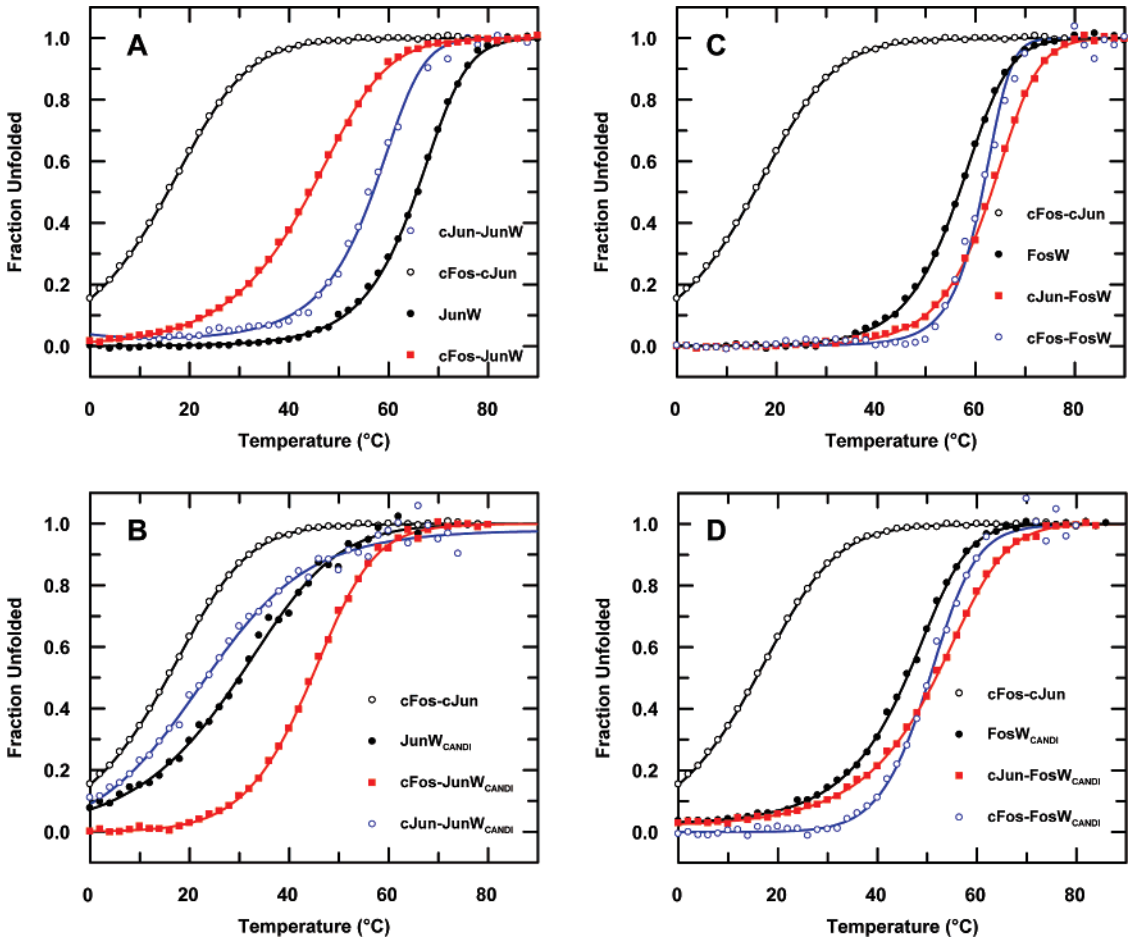

FIGURE 3: Thermal stability of peptide pairs measured by using temperature dependence of the CD signal at 222 nm. In this diagram, wild-type cJun−cFos is represented by black empty circles, the desired complexes are represented by red filled squares, and competing nondesired states are represented by black filled circles and blue empty circles; lines represent fits to the data according to a two-state model (eq 1). In (A) are data for the original JunW, without competitive negative design strategy (*21*). The desired cFos−JunW (red filled squares), although clearly preferential over wild-type cJun−cFos (black empty circles), displays a lower T_m than competing complexes JunW−JunW (black filled circles) and cJun−JunW (blue empty circles). The stability of these complexes however is relieved in (B), where cFos is present as a competitor, resulting in both stability and specificity for the cFos−JunW$_{CANDI}$ complex. The same strategy was attempted for a specific FosW in (C). However, although the T_m of the competing species was compromised, that same was observed in the cJun−FosW$_{CANDI}$ complex in (D). As predicted, the residue variations at specific positions were not sufficient in being able to direct a favorable desired interaction at the detriment of competing states.

positive and thus are predicted to interact well with the negatively charged Glu's of the corresponding cFos were not changed. Only the uncharged ***e3*** Ala would appear to be a poor residue at this position and was replaced with charged (Arg, Lys) as well as polar (Gln) options. cJun ***g*** positions were also varied to retain wild-type residues but also to include charged and polar options.

In the case of JunW$_{CANDI}$, four out of ten possible changes were observed between JunW$_{CANDI}$ and the previously identified JunW (Figure 2A). Of these four changes, three were in electrostatic ***g/e*** positions, and one was at an ***a*** position. Further inspection of these changes using heptad repeat diagrams (Figure 2A−C; see legend for schematic explanation) indicated that increased predicted g_i/e_{i+1} electrostatic repulsions are indeed observed in competing states cJun−JunW$_{CANDI}$ and even more so in JunW$_{CANDI}$−JunW$_{CANDI}$, relative to cJun−JunW and JunW−JunW (Figure 2B,C), respectively. Electrostatic ***g/e*** pairs are similar for cFos−JunW and cFos−JunW$_{CANDI}$ (Figure 2A) and contain no disfavored pairing predictions (*21*, *34*). However, for cJun−JunW → cJun−JunW$_{CANDI}$ (Figure 2B) unfavorable $R_{e4}E_{g3}$ → $R_{e4}K_{g3}$ pairings (according to Krylov *et al.* this gives $\Delta\Delta G$ = +1.3 kcal/mol) and $Q_{g2}Q_{e3}$ → $Q_{g2}R_{e3}$ ($\Delta\Delta G$ = +0.5 kcal/mol (*34*)) changes are observed representing an overall unfavorable energy change of +1.8 kcal/mol. Additionally for JunW−JunW → JunW$_{CANDI}$−JunW$_{CANDI}$ homodimers (Figure 2C) $E_{g3}R_{e4}$ → $K_{g3}R_{e4}$ ($\Delta\Delta G$ = +1.3 kcal/mol (*34*)), $E_{g2}Q_{e3}$ → $E_{g2}R_{e3}$ ($\Delta\Delta G$ = −0.9 kcal/mol (*34*)), $Q_{e3}E_{g2}$ → $R_{e3}E_{g2}$ ($\Delta\Delta G$ = −0.9 kcal/mol (*34*)), and $R_{e4}E_{g3}$ → $R_{e4}K_{g3}$ ($\Delta\Delta G$ = +1.3 kcal/mol (*34*)) are observed, representing an overall unfavorable energy change of some +0.8 kcal/mol. Further specificity comes from core changes predicted to be energetically comparable (TV → TA; cFos−JunW → cFos−JunW$_{CANDI}$; no free energy determined) for the desired species relative to unfavorable VV → VA (for cJun−JunW → cJun−JunW$_{CANDI}$; $\Delta\Delta G$ = +3.1 kcal/mol (*35*)) and VV → AA (for JunW−JunW → JunW$_{CANDI}$−JunW$_{CANDI}$; $\Delta\Delta G$ = +5.4 kcal/mol (*35*)). As a result, the designed state remains more or less unchanged whereas the competing states are disfavored.

To experimentally verify these energetic predictions, thermal denaturation analyses were carried out to provide T_m values for both PCA and CANDI−PCA derived helices alone or in complex with target or competitor. Ellipticity,

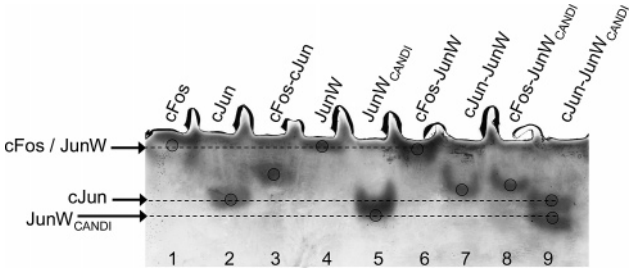

FIGURE 4: A native gel performed at 4 °C demonstrating species that have been designed to form heterotypic complexes. Wild-type cFos−cJun (lane 3) appears as an average of its constituents, cFos (lane 1) and cJun (lane 2). cFos−JunW (lane 6), cannot be distinguished from cFos (lane 1) or JunW (lane 4) due to similarities in isoelectric point. cFos−JunW$_{CANDI}$ (lane 8) clearly forms a heterotypic complex, as it is distinct from its constituents, cFos (lane 1) or JunW$_{CANDI}$ (lane 5). CANDI is shown to be successful by comparison of cJun−JunW (lane 7) and cJun−JunW$_{CANDI}$ (lane 9). While the former clearly forms a heterotypic complex from its constituents, the latter forms two distinct bands which correspond to its components cJun (lane 2) and JunW$_{CANDI}$ (lane 5), thus proving that CANDI is successful at generating the necessary specificity for its cFos target in the presence of a cJun competitor. This is consistent with T_m data (Figure 3), with a ΔT_m of −34 °C for cJun−JunW$_{CANDI}$ relative to cJun−JunW (Table 1). A plot of charge vs pH (not shown) explains the migration patterns for the peptides at pH 3.8.

corresponding to helical content, was monitored as a function of temperature (see Figure 3). Each of the profiles fit to a two-state model, where only the unfolded and folded states are significantly populated (see Materials and Methods). While the melting data of winner peptides, derived with and without CANDI, led to indiscriminable T_m's for the cFos−JunW (T_m = 44 °C) and cFos−JunW$_{CANDI}$ (T_m = 44 °C) complexes (ΔT_m = 0), the stabilities of JunW$_{CANDI}$ homodimer (T_m = 29 °C) and cJun−JunW$_{CANDI}$ (T_m = 23 °C) complexes were severely impaired relative to JunW−JunW (T_m = 66 °C) and cJun−JunW (T_m = 57 °C), with ΔT_m's of −37 °C and −34 °C, respectively (Table 1). It should be noted that although some complexes display higher T_m's, it does not necessarily imply that they are favored when all species are present in solution. For example, JunW−JunW has a higher T_m than either cFos−cFos or cFos−JunW, but the latter is favored when all three helices are mixed because the instability of cFos drives heterodimerization. This is similar to a mixture of the wild-type cFos and cJun species; cFos−cFos is unstable and unable to homodimerize under native conditions, meaning that the resulting high monomeric cFos concentration pushes the equilibrium in favor of a cFos−cJun heterodimer over cJun−cJun dimers and unfolded cFos (*37*).

Resulting ΔT_m values were converted into free energy differences (see Mason et al. 2006 (*21*) and Materials and Methods). Most core and electrostatic interaction changes could be estimated from the literature (*34*, *35*), and these values are found to agree reasonably well with the calculated free energy changes. Undesired species (JunW homodimers and complexes with cJun) were destabilized relative to desired complexes (with cFos) in both calculated ($\Delta\Delta G$ = +6.2 and +4.8 vs −0.9 kcal/mol) and measured values ($\Delta\Delta G$ = +5.2 and +4.9 vs −0.7 kcal/mol). These values highlight that calculation based basic pairing rules are feasible within certain error margins, but more work is needed in teasing specificity from stability based rules. Importantly, using CANDI we were able to improve the free energy difference between nondesired and desired species by 5.9 kcal/mol or 5.6 kcal/mol, respectively, while the free energy of the cFos−JunW$_{CANDI}$ complex exceeds the wild-type cFos−cJun interaction by 3.2 kcal/mol.

Native gel electrophoresis was applied to visualize increased specificity (Figure 4). In this experiment, gels lacking SDS permit fully folded peptides to migrate according to their overall charge at low pH. This in turn permits homodimeric complexes to be distinguished from those which are heterodimeric. For example, wild-type cFos−cJun (lane 3) appears as an average of its constituents, cFos (lane 1) and cJun (lane 2). The heterotypic cFos−JunW (lane 6) cannot be distinguished from cFos (lane 1) or JunW (lane 4) due to similarities in isoelectric point, but thermal melting data (Table 1) demonstrates the T_m of this heterodimer to far exceed the average of its homodimeric constituents indicating favored heterodimeric formation. cFos−JunW$_{CANDI}$ (lane 8) clearly forms a heterotypic complex, as it is distinct from its constituents, cFos (lane 1) or JunW$_{CANDI}$ (lane 5). Strong evidence for the validity of CANDI comes from comparison of cJun−JunW (lane 7) and cJun−JunW$_{CANDI}$ (lane 9); while the former clearly forms a heterotypic complex from its constituents, the latter forms two distinct bands which correspond to its components cJun (lane 2) and JunW$_{CANDI}$ (lane 5), thus proving that CANDI was successful at generating the necessary specificity for its cFos target in the presence of the cJun competitor. Despite an apparent two-state unfolding profile during thermal melting of cJun−JunW$_{CANDI}$ (Figure 3), the observed curve is however consistent with concomitant independent unfolding of the two respective homodimers that were observed in the native gel. Indeed, the average of the two homodimeric T_m's is very close to the observed T_m (Table 1).

A further CD-based experiment looked at peptide exchange in preformed complexes. In mixing cJun−cJun complexes (Figure 5A, red line, T_m 24 °C) and cFos−JunW$_{CANDI}$ complexes (Figure 5A, yellow line, T_m 44 °C), one would predict the latter to be favored. In doing so, the remaining cJun helices would be expected to remain in their homodimeric form. This is indeed observed, and we see a superimposition of the calculated summed (Figure 5A; black hash) against the observed (Figure 5A, orange line) CD spectra for the mixture. Conversely, the summed CD signals (Figure 5B, black hash) for premixed cJun−cFos (Figure 5B, red line, T_m 16 °C) and cJun−JunW$_{CANDI}$ (Figure 5B, yellow line T_m 23 °C) would not be predicted to materialize because the peptides would exchange to form the more stable cFos−JunW$_{CANDI}$, leaving the free cJun to homodimerize. This was indeed observed (Figure 5B, orange line) and once again demonstrates JunW$_{CANDI}$ to be highly specific for cFos in the presence of cJun.

Differences between FosW and FosW$_{CANDI}$. For this selection, the coiled coil region of cJun was used as target, with the library based on cFos. The core of cFos is significantly impaired. It cannot homodimerize and binds with an apparent weak K_D *in vivo* (*37*−*39*) which may reflect the biological requirement for the complex. For designing inhibitors of maximal specificity and stability wild-type ***a*** residues were replaced with Leu, Val, and Ile options; ***a3*** alone was locked to Asn to generate an interhelical hydrogen bond with cJun, aiding in maintaining correct periodicity and

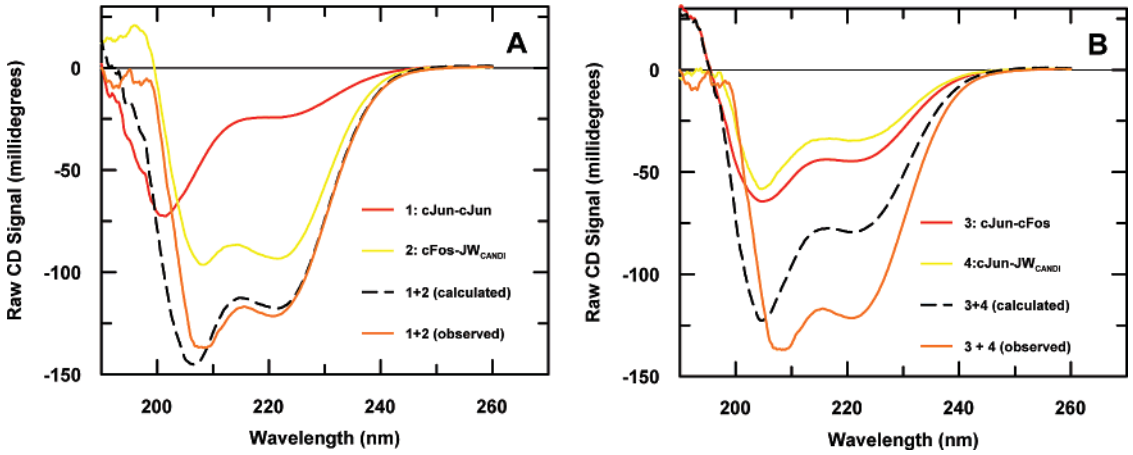

FIGURE 5: Dimer exchange as a measure of specificity. Four individual helices (75 μM per monomer; 150 μM per homo/heterodimer; 300 μM total peptide) were mixed at 20 °C as for previous CD experiments, at the same volume (250 μL) in a 1 mm path length CD cell. (A) Mixing of cJun−cJun (red; T_m 24 °C) and cFos−Jun$_{CANDI}$ (yellow; T_m 44 °C) would be predicted to favor the latter, with remaining cJun helices free to homodimerize. This is indeed observed, with the superimposition of the calculated summed data (black hash) with the observed helix mixture (orange). (B) Conversely the summed CD signals for cJun−cFos (red; T_m 16 °C) and cJun−JunW$_{CANDI}$ (yellow; T_m 23 °C) do not superimpose (black hash) with the observed mixture (orange) because the monomers exchange to the earlier scenario.

orientation (*40*) (Figure 2D). The remaining nine positions, all of which are found at the solvent exposed positions, are options from homologues FosB, Fra1, Fra2, and dFra, and again represent subtle and sometimes unintuitive changes which have been shown to be preferred over the wild-type options (*21*), possibly because of an increased helical propensity to which they collectively contribute. Owing to the residue options available to the Fos library, as well as uncommon ***g/e*** cJun residues, repulsive options for competing energetic states were severely limited, and CANDI was not predicted to be of success for this particular library.

In the case of FosW$_{CANDI}$, six of a possible thirteen residues differed from the previous winner (termed FosW, see Figure 2D). Of these changes, four of a possible four were in electrostatic ***g/e*** positions and one of a possible four was at an ***a*** position (see Figure 2D−F). For example, FosW−cJun → FosW$_{CANDI}$−cJun, $R_{g2}A_{e3} \rightarrow Q_{g2}A_{e3}$ ($\Delta\Delta G = -0.2$ kcal/mol (*34*)) and $R_{e3}Q_{g2} \rightarrow Q_{e3}Q_{g2}$ ($\Delta\Delta G = -0.5$ kcal/mol (*34*)) changes in the desired interaction are almost entirely matched by $R_{g2}Q_{e3} \rightarrow Q_{g2}Q_{e3}$ ($\Delta\Delta G = -0.5$ kcal/mol (*34*)), $R_{e3}E_{g2} \rightarrow Q_{e3}E_{g2}$ ($\Delta\Delta G = +0.9$ kcal/mol (*34*)), and $Q_{e4}E_{g3} \rightarrow R_{e4}E_{g3}$ ($\Delta\Delta G = -0.9$ kcal/mol (*34*)) changes. Finally for the FosW−FosW → FosW$_{CANDI}$−FosW$_{CANDI}$ change, electrostatic stabilization from two times $E_{g3}Q_{e4} \rightarrow E_{g3}R_{e4}$ ($\Delta\Delta G = -1.7$ kcal/mol (*34*)) and $R_{g2}R_{e3} \rightarrow Q_{g2}Q_{e3}$ ($\Delta\Delta G = -2.2$ kcal/mol (*34*)) is predicted. Despite this, the T_m of the homodimeric competing state is not seen to increase when CANDI is introduced. Indeed these thermal melt analyses demonstrated all three complexes to have significantly compromised stabilities with CANDI relative to PCA. This is possibly explained by the single Ile → Ala (at ***a4*** of cFos and cJun, respectively), and it is interesting to note that only one of the four possible ***a*** options were changed for FosW$_{CANDI}$ relative to FosW, and that this change was not sufficient to direct specificity. This core change was predicted to be destabilizing in the desired FosW$_{CANDI}$−cJun species relative to FosW−cJun (IA → VA, $\Delta\Delta G = +1.8$ kcal/mol (*35*)). However, in contrast to the electrostatics, the core changes in the competing complexes were predicted to be more unfavorable by comparison (II → VI, $\Delta\Delta G = +3.0$ kcal/mol; II → VV, $\Delta\Delta G = +3.8$ kcal/mol (*35*)). This negative design strategy clearly lacked the electrostatic and core options able to collectively impose specificity upon the library winner. Of the changes made, all would be predicted to make comparable free energy contributions (*21*, *34*). The summed energetic data calculated from the literature (*34*, *35*) also show good agreement with measured free energy changes from thermal unfolding/refolding data. Undesired (homodimers and complexes with cFos) and desired species (complexes with cJun) are destabilized in both calculated ($\Delta\Delta G = -0.1$ and $+2.5$ kcal/mol vs $+1.2$ kcal/mol) and measured ($\Delta\Delta G = +2.2$ and $+3.6$ kcal/mol vs $+3.1$ kcal/mol) values. Although the overall order of stabilities is correctly predicted, a wealth of experimental data will be required in further refining these predictions.

DISCUSSION

Understanding how nature has evolved structurally similar proteins to be able to bind uniquely and with high affinity to another represents an important biological question. There have been several previous investigations into this question; Havranek and Harbury (*24*) demonstrated positive and negative design using a multistate *in silico* approach with *in vitro* testing. Adding unfavorable competing interactions, overlooked in single-state design, ruled out potential free energy minima or traps arising from nonspecific pairings, generating improved specificity in a GCN4 derived scaffold with residue pairs rarely observed in coiled coil design. Similarly, Alber's group implemented heterospecificity and negative design using a computational approach (*41*, *42*). Likewise, Woolfson's group has used positive and negative design by strategically placing polar and charged residues to generate self-assembling coiled coil based nanoparticles (*43*). Positions at the subunit−subunit interface of the SspB adaptor protein were randomized using the ORBIT code (*44*) with and without negative design. Changes optimizing the stability of the target species were speculated to have random energetic effects on nontarget conformations, making explicit negative design unnecessary. However, only the negative computational design resulted in urea denaturation profiles where heterodimers were significantly stabilized over homodimers. This was achieved by maximizing the energetic

gap between these species, with a fixed backbone assumed to reduce computing time.

We have addressed the question of how specificity is achieved by using libraries to select peptides which must bind with high affinity to their target, and compared them to those which must bind with high affinity *and* specificity to the same target. The latter has been achieved by the addition of competing peptides that act to mimic natural evolution. This is therefore an important addition to the selection toolbox. PCA has been used to select binding partners for numerous examples and in different systems (*1*, *10*, *21*, *28*−*30*). We have introduced a *competitive and negative design initiative* into the PCA selection process, and consequently termed this advanced system CANDI−PCA. A direct comparison between both systems revealed that CANDI−PCA is clearly superior in simultaneously generating stable *and* highly specific peptides. Although the conventional PCA system already encompassed a degree of negative design (outcomes 2 and 3 in Figure 1), selection pressure apparently was not high enough to prevent a mixture of outcomes 1 and 3 in the conventional PCA selection. Considerable homodimer formation of library members was observed (see also Figure 3A). In contrast in CANDI−PCA, the addition of a specific competitor of high similarity (i.e., another closely related coiled coil motif) expressed to high concentrations on a separate plasmid generated an additional level of selection pressure. Indeed, selected $JunW_{CANDI}$ homodimers as well as $JunW_{CANDI}$−cJun heterodimers are destabilized relative to the desired $JunW_{CANDI}$−cFos interaction.

Specifically, 37-mer peptides ($JunW_{CANDI}$, JunW) are able to target cFos equally well (T_m = 44 °C), and with significant improvement over the wild-type complex (cFos−cJun; T_m = 16 °C (*21*)). Remarkably, huge differences were observed when comparing the competing interactions cJun−JunW (T_m = 57 °C) and JunW homodimer (T_m = 66 °C) with only the instability of the wild-type complex partially driving the desired species formation (*21*, *37*). Contrastingly, $JunW_{CANDI}$ showed significantly lower stabilities in these competing states ($JunW_{CANDI}$−cJun T_m = 23 °C; $JunW_{CANDI}$ homodimeric T_m = 29 °C) leaving the target interaction 5.6 kcal mol^{-1} more stable than the most stable nondesired species. The bulk of this unfavorable free energy difference is attained via core packing variations and nonoptimal electrostatic pairings for undesired complexes, with comparably favorable interactions for desired species obtained with either PCA or CANDI−PCA. This confirms the hypothesis that was raised in the introduction, namely, that negative design is important for generation of high specificity, and that it cannot be achieved as a byproduct of optimizing for stability alone. Specificity would appear to be driven by both the hydrophobic core residues, as well as core flanking electrostatic contributions, both of which were predicted to be less favorable for residue pairings in the competing species relative to the desired species (Figure 2A−C). This is in good agreement with free energy values obtained from thermal data (Figure 3). Further, a coiled coil prediction algorithm (bCIPA; http://www.molbiotech.uni-freiburg.de/bCIPA (*21*)) based on a previous study of 57 bZIP interactions was correct in predicting the overall rank for $JunW_{CANDI}$, but was less impressive in predicting the $FosW_{CANDI}$ containing complexes, possibly reflecting an overweighted core consideration in the algorithm (*21*) for this non-native helix. Finally, with a T_m of 44 °C for both JunW and $JunW_{CANDI}$, it is puzzling as to why selecting for specificity did not compromise affinity. One might speculate this to be due to a shift in the equilibria imposed by the presence of the competing helix, with a corresponding change in the kinetics contributing to this equilibrium. Alternatively, $JunW_{CANDI}$ may not have been selected in the first instance owing to biophysically uncharacterized reasons, for example cellular effects such as subtle differences in solubility or protease resistance.

Including residue options designed to potentially lower the stability of the desired complex will increase the likelihood of identifying a compromised sequence that can bind its target, while ruling out the formation of undesirable pairs of similar free energy. Indeed, $JunW_{CANDI}$ was able to successfully circumvent the four detrimental outcomes proposed in the introduction because it had the residue repertoire able to bind specifically to cFos. In contrast in the case of $FosW_{CANDI}$, clones were observed and grew in M9 minimal media but no increased specificity was observed with any of the biophysical methods of analysis. This is in total agreement with our prediction that the Fos library was lacking suitable residues to bind with high affinity and specificity. This demonstrates that specificity is a tradeoff for stability, and that one cannot optimize one without compromising the other.

With the lack of computer processing time hindering the *in silico* search for specificity, *in vivo* design remains a powerful alternative in the design of specific, stable peptide-based drugs, and for providing information for computationalists to generate the necessary rules to speed up the search for new drugs. We targeted the coiled coil domain of the oncogenic proteins cJun and cFos, and obtained a set of AP-1 directed peptides which will be useful in downregulating AP-1 activity in tumor cells. These have the potential to serve as lead compounds in innovative drug design. For improved half-lives, the transfer of such an assay to a mammalian cell line containing therapeutically relevant proteases, as well as expression of an array of other peptides, may well be the way forward, with peptidomimetic constructs of the winner likely to be the end result. Proof of principle for the PCA assay in the mammalian Chinese hamster ovary cell line has already been demonstrated (*45*, *46*). Experimentalists can therefore harness nature to impose stringently and precisely the rules that computational biophysicists must approximate to using selected competitor sequences, in addition to significant amounts of computing time.

Unlike computational design algorithms (*24*, *44*), no approximations or assumptions such as fixed backbone limitations or side-chain geometry estimates are necessary for this CANDI−PCA approach. The *in vivo* assay generates "winning" helices which already fulfill the criteria that are required of them. It should be emphasized that although we have used PCA to monitor protein−protein interactions, CANDI is however completely adaptable and is equally applicable in other *in vivo* protein−protein interaction systems such as the yeast two-hybrid or lambda repressor system. Moreover, optimization can be achieved by inclusion of options designed to generate compromised intermolecular contacts in the desired species. This is an overlooked prerequisite in libraries designed to generate peptides that are specific for their target. Inclusion of such residues, in

addition to those predicted to be favorable for the desired interaction, act to specify protein−protein interactions which are stable, while ensuring that otherwise energetically accessible alternatives are not. We have shown that for the coiled coil system specificity is achieved using a combination of hydrophobic and electrostatic differences, both of which make little difference to the affinity of the desired interaction but impose large energetic penalties on competing states. For example, this has been observed in the context of buried polar (Asn−Asn) pairings which, although destabilizing, have been shown to incur a larger energetic penalty if the hydrogen bond is unsatisfied (*40*). The ultimate aim is the generation of new rules, and to promote understanding of coiled coil cross-talk in cells, allowing design of high affinity and specificity, from the outset. These data will contribute to the understanding of how natural evolution generates specificity and diversity, as well as being an essential prerequisite in designing peptide-based drugs with minimal cross-talk.

ACKNOWLEDGMENT

The authors wish to thank Karin Schmidtkunz for excellent technical assistance throughout.

REFERENCES

1. Dobson, C. M. (2003) Protein folding and misfolding, *Nature 426*, 884−90.
2. Wolf, E., Kim, P. S., and Berger, B. (1997) MultiCoil: a program for predicting two- and three-stranded coiled coils, *Protein Sci. 6*, 1179−89.
3. Glover, J. N., and Harrison, S. C. (1995) Crystal structure of the heterodimeric bZIP transcription factor c-Fos-c-Jun bound to DNA, *Nature 373*, 257−61.
4. Brown, J. H., Cohen, C., and Parry, D. A. (1996) Heptad breaks in alpha-helical coiled coils: stutters and stammers, *Proteins 26*, 134−45.
5. Xu, Y., Zhu, J., Liu, Y., Lou, Z., Yuan, F., Liu, Y., Cole, D. K., Ni, L., Su, N., Qin, L., Li, X., Bai, Z., Bell, J. I., Pang, H., Tien, P., Gao, G. F., and Rao, Z. (2004) Characterization of the heptad repeat regions, HR1 and HR2, and design of a fusion core structure model of the spike protein from severe acute respiratory syndrome (SARS) coronavirus, *Biochemistry 43*, 14064−71.
6. Bianchi, E., Finotto, M., Ingallinella, P., Hrin, R., Carella, A. V., Hou, X. S., Schleif, W. A., Miller, M. D., Geleziunas, R., and Pessi, A. (2005) Covalent stabilization of coiled coils of the HIV gp41 N region yields extremely potent and broad inhibitors of viral infection, *Proc. Natl. Acad. Sci. U.S.A. 102*, 12903−8.
7. Sharma, V. A., Logan, J., King, D. S., White, R., and Alber, T. (1998) Sequence-based design of a peptide probe for the APC tumor suppressor protein, *Curr. Biol. 8*, 823−30.
8. Siegert, R., Leroux, M. R., Scheufler, C., Hartl, F. U., and Moarefi, I. (2000) Structure of the molecular chaperone prefoldin: unique interaction of multiple coiled coil tentacles with unfolded proteins, *Cell 103*, 621−32.
9. Kitamura, K., Tanaka, H., and Nishimune, Y. (2005) The RING-finger protein haprin: domains and function in the acrosome reaction, *Curr. Protein Pept. Sci. 6*, 567−74.
10. Yu, Y. B. (2002) Coiled-coils: stability, specificity, and drug delivery potential, *Adv. Drug Delivery Rev. 54*, 1113−29.
11. Mason, J. M., and Arndt, K. M. (2004) Coiled coil domains: stability, specificity, and biological implications, *ChemBioChem 5*, 170−6.
12. Woolfson, D. N. (2005) The design of coiled-coil structures and assemblies, *Adv. Protein Chem. 70*, 79−112.
13. Mason, J. M., Müller, K. M., and Arndt, K. M. (2007) Considerations in the Design and Optimization of Coiled coil Structures, *Methods Mol. Biol. 352*, 35−70.
14. Müller, K. M., Arndt, K. M., and Alber, T. (2000) Protein fusions to coiled-coil domains, *Methods Enzymol. 328*, 261−82.
15. Arndt, K. M., Müller, K. M., and Plückthun, A. (2001) Helix-stabilized Fv (hsFv) antibody fragments: substituting the constant domains of a Fab fragment for a heterodimeric coiled-coil domain, *J. Mol. Biol. 312*, 221−8.
16. Pandya, M. J., Cerasoli, E., Joseph, A., Stoneman, R. G., Waite, E., and Woolfson, D. N. (2004) Sequence and structural duality: designing peptides to adopt two stable conformations, *J. Am. Chem. Soc. 126*, 17016−24.
17. Schnarr, N. A., and Kennan, A. J. (2003) Specific control of peptide assembly with combined hydrophilic and hydrophobic interfaces, *J. Am. Chem. Soc. 125*, 667−71.
18. Lupas, A. N., and Gruber, M. (2005) The structure of alpha-helical coiled coils, *Adv. Protein Chem. 70*, 37−78.
19. Eferl, R., and Wagner, E. F. (2003) AP-1: a double-edged sword in tumorigenesis, *Nat. Rev. Cancer 3*, 859−68.
20. Libermann, T. A., and Zerbini, L. F. (2006) Targeting transcription factors for cancer gene therapy, *Curr. Gene Ther. 6*, 17−33.
21. Mason, J. M., Schmitz, M. A., Müller, K. M., and Arndt, K. M. (2006) Semirational design of Jun-Fos coiled coils with increased affinity: Universal implications for leucine zipper prediction and design, *Proc. Natl. Acad. Sci. U.S.A. 103*, 8989−94.
22. Nomura, Y., and Yokobayashi, Y. (2006) Dual selection of a genetic switch by a single selection marker, *Biosystems*, in press.
23. Collins, C. H., Leadbetter, J. R., and Arnold, F. H. (2006) Dual selection enhances the signaling specificity of a variant of the quorum-sensing transcriptional activator LuxR, *Nat. Biotechnol. 24*, 708−12.
24. Havranek, J. J., and Harbury, P. B. (2003) Automated design of specificity in molecular recognition, *Nat. Struct. Biol. 10*, 45−52.
25. Pelletier, J. N., Arndt, K. M., Plückthun, A., and Michnick, S. W. (1999) An in vivo library-versus-library selection of optimized protein-protein interactions, *Nat. Biotechnol. 17*, 683−90.
26. Pelletier, J. N., Campbell-Valois, F. X., and Michnick, S. W. (1998) Oligomerization domain-directed reassembly of active dihydrofolate reductase from rationally designed fragments, *Proc. Natl. Acad. Sci. U.S.A. 95*, 12141−6.
27. Arndt, K. M., Pelletier, J. N., Müller, K. M., Alber, T., Michnick, S. W., and Plückthun, A. (2000) A heterodimeric coiled-coil peptide pair selected in vivo from a designed library-versus-library ensemble, *J. Mol. Biol. 295*, 627−39.
28. Arndt, K. M., Pelletier, J. N., Müller, K. M., Plückthun, A., and Alber, T. (2002) Comparison of in vivo selection and rational design of heterodimeric coiled coils, *Structure 10*, 1235−48.
29. Nyfeler, B., Michnick, S. W., and Hauri, H. P. (2005) Capturing protein interactions in the secretory pathway of living cells, *Proc. Natl. Acad. Sci. U.S.A. 102*, 6350−5.
30. Koch, H., Grafe, N., Schiess, R., and Plückthun, A. (2006) Direct selection of antibodies from complex libraries with the protein fragment complementation assay, *J. Mol. Biol. 357*, 427−41.
31. Du, H., Fuh, R. A., Li, J., Corkan, A., and Lindsey, J. S. (1998) PhotochemCAD: A computer-aided design and research tool in photochemistry, *Photochem. Photobiol. 68*, 141−142.
32. Zitzewitz, J. A., Bilsel, O., Luo, J., Jones, B. E., and Matthews, C. R. (1995) Probing the folding mechanism of a leucine zipper peptide by stopped-flow circular dichroism spectroscopy, *Biochemistry 34*, 12812−9.
33. Sosnick, T. R., Jackson, S., Wilk, R. R., Englander, S. W., and DeGrado, W. F. (1996) The role of helix formation in the folding of a fully alpha-helical coiled coil, *Proteins 24*, 427−32.
34. Krylov, D., Barchi, J., and Vinson, C. (1998) Inter-helical interactions in the leucine zipper coiled coil dimer: pH and salt dependence of coupling energy between charged amino acids, *J. Mol. Biol. 279*, 959−72.
35. Acharya, A., Ruvinov, S. B., Gal, J., Moll, J. R., and Vinson, C. (2002) A heterodimerizing leucine zipper coiled coil system for examining the specificity of a position interactions: amino acids I, V, L, N, A, and K, *Biochemistry 41*, 14122−31.
36. Bosshard, H. R., Durr, E., Hitz, T., and Jelesarov, I. (2001) Energetics of coiled coil folding: the nature of the transition states, *Biochemistry 40*, 3544−52.

37. O'Shea, E. K., Rutkowski, R., and Kim, P. S. (1992) Mechanism of specificity in the Fos-Jun oncoprotein heterodimer, *Cell 68*, 699−708.
38. Olive, M., Krylov, D., Echlin, D. R., Gardner, K., Taparowsky, E., and Vinson, C. (1997) A dominant negative to activation protein-1 (AP1) that abolishes DNA binding and inhibits oncogenesis, *J. Biol. Chem. 272*, 18586−94.
39. Boysen, R. I., Jong, A. J., Wilce, J. A., King, G. F., and Hearn, M. T. (2002) Role of interfacial hydrophobic residues in the stabilization of the leucine zipper structures of the transcription factors c-Fos and c-Jun, *J. Biol. Chem. 277*, 23−31.
40. Gonzalez, L., Jr., Woolfson, D. N., and Alber, T. (1996) Buried polar residues and structural specificity in the GCN4 leucine zipper, *Nat. Struct. Biol. 3*, 1011−8.
41. Nautiyal, S., Woolfson, D. N., King, D. S., and Alber, T. (1995) A designed heterotrimeric coiled coil, *Biochemistry 34*, 11645−51.
42. Nautiyal, S., and Alber, T. (1999) Crystal structure of a designed, thermostable, heterotrimeric coiled coil, *Protein Sci. 8*, 84−90.
43. Ryadnov, M. G., Ceyhan, B., Niemeyer, C. M., and Woolfson, D. N. (2003) "Belt and braces": a peptide-based linker system of de novo design, *J. Am. Chem. Soc. 125*, 9388−94.
44. Bolon, D. N., Grant, R. A., Baker, T. A., and Sauer, R. T. (2005) Specificity versus stability in computational protein design, *Proc. Natl. Acad. Sci. U.S.A. 102*, 12724−9.
45. Remy, I., and Michnick, S. W. (1999) Clonal selection and in vivo quantitation of protein interactions with protein-fragment complementation assays, *Proc. Natl. Acad. Sci. U.S.A. 96*, 5394−9.
46. Leveson-Gower, D. B., Michnick, S. W., and Ling, V. (2004) Detection of TAP family dimerizations by an in vivo assay in mammalian cells, *Biochemistry 43*, 14257−64.

BI602506P